Journal Name

ARTICLE TYPE

Cite this: DOI: 00.0000/xxxxxxxxxx

Acoustic phonon-restricted four-phonon interactions: Impact on thermal and thermoelectric transport in monolayer h−NbN

Himanshu Murari [a], Subhradip Ghosh [a], Mukul Kabir [b], and Ashis Kundu *[b]

Received Date
Accepted Date

DOI: 00.0000/xxxxxxxxxx

Supporting Information

1 Convergence test of κ_l

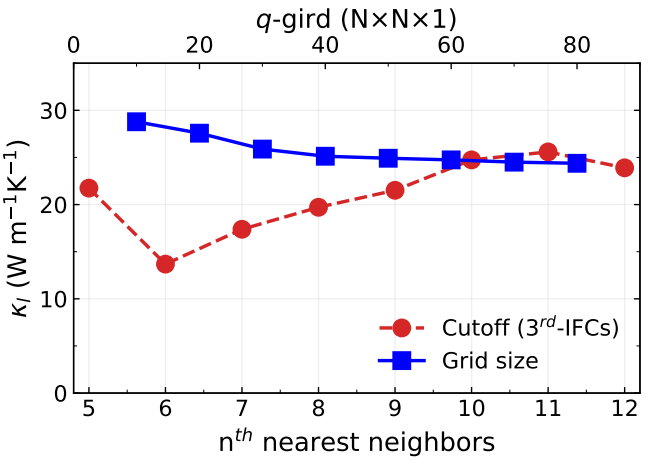

Fig. S1 Calculated lattice thermal conductivity (κ_l) at 300 K as a function of the n^{th} nearest neighbor cutoff for third-order interatomic force constants (IFCs) and the q-grid size (N×N×1). The difference in κ_l between the 10th and 11th neighbors, and between the 10th and 12th neighbors, is less than 5%. Thus, convergence is achieved at the 10^{th} nearest neighbor cutoff with a $60 \times 60 \times 1$ q-grid.

2 Thermodynamic stability

We have verified the thermodynamical stability through *ab initio* molecular dynamics (AIMD) simulations (performed with the VASP code) for h-NbN at 300 K, 600 K, and 800 K. The AIMD simulations are performed using the canonical ensemble (NVT) in the Nosé-Hoover heat bath. A 4×4×1 supercell with a 1×1×1 k-grid is used for these calculations. Figure S2 shows the variation in free energy (red) and temperature (blue), with an inset showing the initial and final structure of h-NbN (top view). The free energy and temperature fluctuate around stable mean values throughout the 15-ps simulation time, and no signs of bond breaking and structural phase transitions are observed. Hence, this confirms the thermodynamic stability at elevated temperatures.

[a] *Department of Physics, Indian Institute of Technology Guwahati, Guwahati-781039, Assam, India*
[b] *Department of Physics, Indian Institute of Science Education and Research, Pune-411008, India, E-mail*: ashiskundu174@gmail.com*

† Electronic Supplementary Information (ESI) available: [details of any supplementary information available should be included here]. See DOI: 00.0000/00000000.

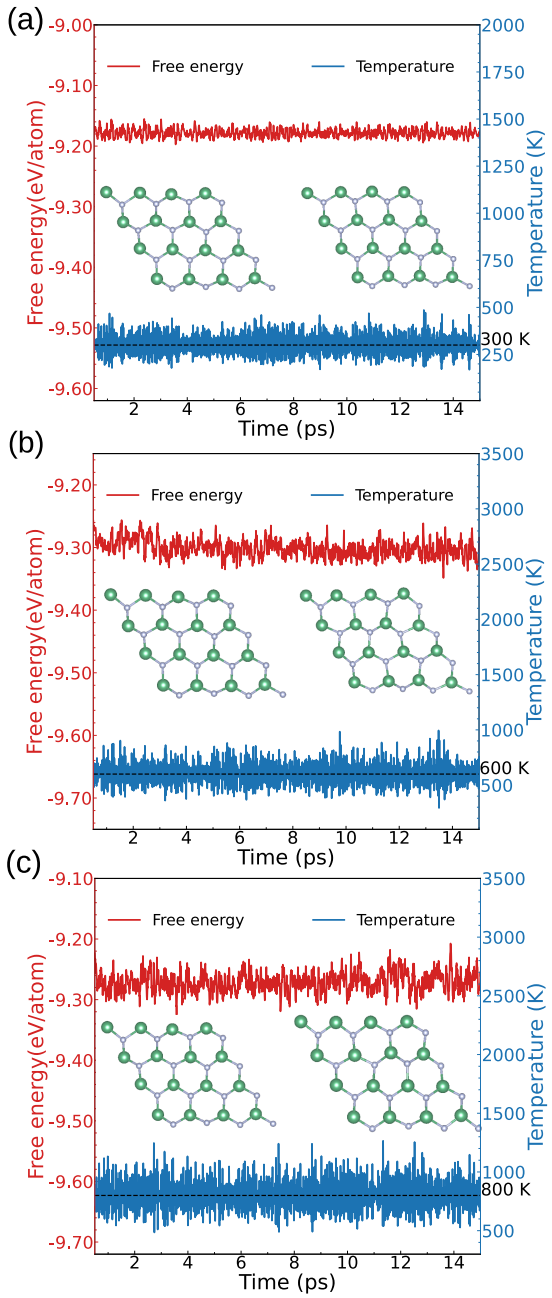

Fig. S2 *Ab initio* molecular dynamics (AIMD) simulations of monolayer h-NbN at (a) 300 K, (b) 600 K, and (c) 800 K over a simulation time of 15 ps.

3 Electronic band structure

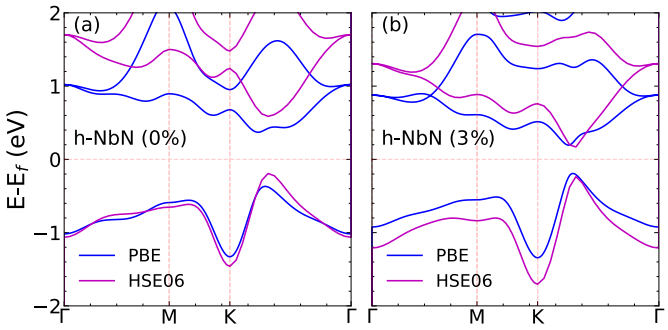

Fig. S3 The electronic band structure (using GGA-PBE and HSE06 functional) reveals an indirect band gap along the $K-\Gamma$ path for both unstrained ($\varepsilon = 0\%$) and strained ($\varepsilon = 3\%$) h−NbN. The band gap decreases under strain. The Fermi level is set to 0 eV.

4 Mode contribution of κ_l and scattering rates

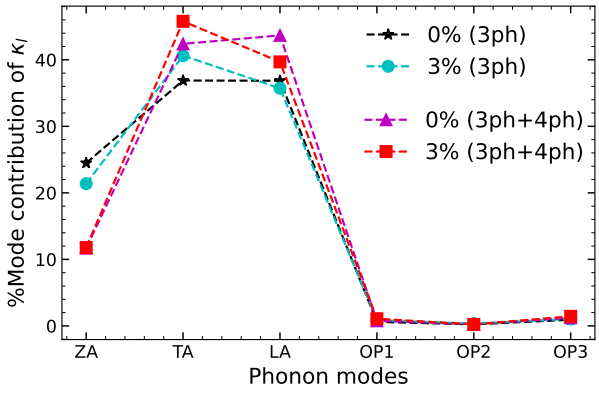

Fig. S4 The percentage contribution of phonon modes to the lattice thermal conductivity (κ_l) reveals that acoustic modes dominate regardless of the scattering order and applied strain. ZA, TA, and LA correspond to the three acoustic modes, while OP1, OP2, and OP3 denote the optical modes.

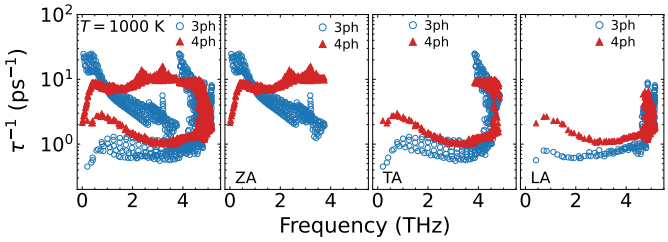

Fig. S5 Comparison of three- and four-phonon scattering reveals that four-phonon processes increase more rapidly with temperature than three-phonon processes. Mode-resolved contributions further clarify this trend, showing that four-phonon scattering in the TA and LA modes surpasses their three-phonon counterparts.

5 Grüneisen parameter (γ)

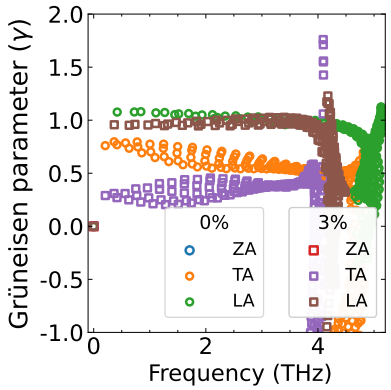

Fig. S6 The Grüneisen parameter (γ) reflects the anharmonicity of the system and is primarily dominated by the ZA mode, which is significantly suppressed under tensile strain (as shown in the main paper). Here, we highlight the suppression of γ for TA and LA modes under strain.

6 Phonon scattering rates and weighted phase space

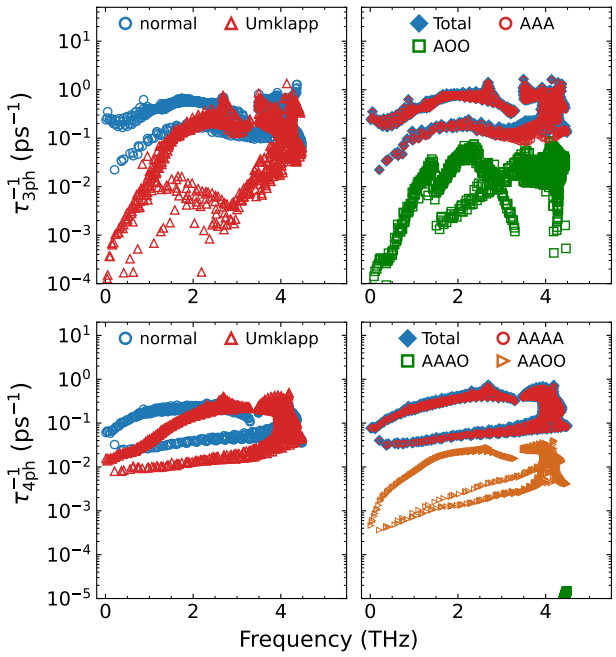

Fig. S7 (a) Three-phonon (3ph) (b) four-phonon (4ph) scattering rates are presented. At 300 K, both three-phonon and four-phonon scattering in monolayer h−NbN are also predominantly governed by normal processes rather than Umklapp scattering under tensile strain 3%. Moreover, phonon scattering is primarily driven by all-acoustic processes, specifically the AAA and AAAA channels.

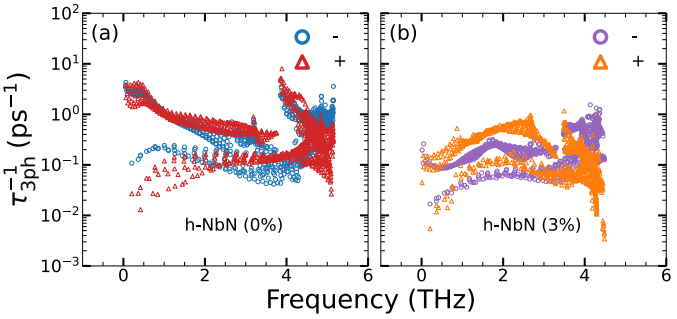

Fig. S8 At 300 K, three-phonon scattering in h−NbN is dominated by absorption (+) processes rather than decay (−) events, under both unstrained and strained conditions.

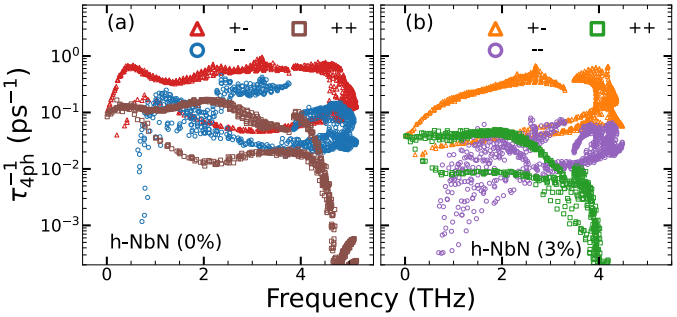

Fig. S9 At 300 K, four-phonon scattering in h−NbN is predominantly governed by redistribution (+−) events over splitting (−−) and recombination (++) events, for both unstrained and strained conditions.

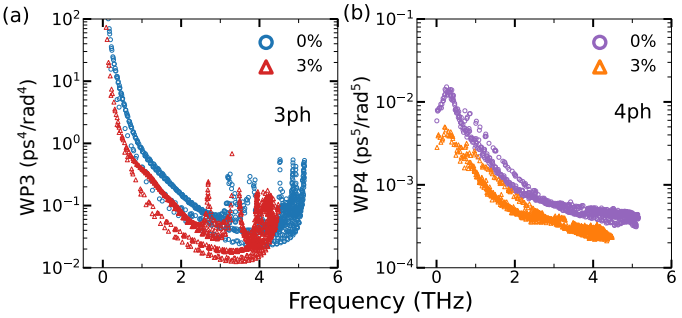

Fig. S10 The weighted phase space for both three- and four-phonon processes decreases under strain, leading to reduced phonon scattering and an increase in lattice thermal conductivity at 300 K.

7 Electron-phonon scattering rates

The electron-phonon averaged (EPA) approach is used to evaluate the carrier relaxation time (τ_{ep}). In the EPA method, explicit averages of electron-phonon scattering rates over the entire Brillouin zone, including all phonon branches and coupling strengths, are considered. The energy-dependent relaxation time is then expressed as:

$$\tau_{ep}^{-1}(\varepsilon,\mu,T) =$$

$$\frac{2\pi\Omega}{g_s\hbar}\sum_{\nu}\Big[g_{\nu}^{2}(\varepsilon,\varepsilon+\bar{\omega}_{\nu})\Big\{n(\bar{\omega}_{\nu},T)+f(\varepsilon+\bar{\omega}_{\nu},\mu,T)\Big\}\rho(\varepsilon+\bar{\omega}_{\nu})$$

$$+g_{\nu}^{2}(\varepsilon,\varepsilon-\bar{\omega}_{\nu})\Big\{n(\bar{\omega}_{\nu},T)+1-f(\varepsilon-\bar{\omega}_{\nu},\mu,T)\Big\}\rho(\varepsilon-\bar{\omega}_{\nu})\Big]$$

Here, ε denotes the carrier energy, μ is the chemical potential, T is the absolute temperature, Ω is the primitive cell volume, $\hbar$ is the reduced Planck constant, g_s is the spin degeneracy, ν represents the phonon mode, g_{ν}^{2} is the averaged electron-phonon matrix element, $\bar{\omega}_{\nu}$ is the average phonon mode energy, $n(\bar{\omega}_{\nu},T)$ is the Bose-Einstein distribution function, $f(\varepsilon,\mu,T)$ is the Fermi-Dirac distribution function, and $\rho(\varepsilon)$ is the electron density of states per unit volume. Further details can be found in Ref. 1

Figure S11 shows the electron-phonon relaxation time (τ_{ep}) as a function of energy for both unstrained and strained h−NbN. It is evident that τ_{ep} obtained from the EPA method strongly depends on the carrier density, unlike the constant relaxation time approximation, highlighting its importance. For both strained and unstrained h−NbN, the τ_{ep} for holes is higher than that for electrons. This behavior can be attributed to the presence of multiple small valleys in the conduction band, which promote stronger electron scattering compared to the relatively non-dispersive valence band, except for a pronounced dip at the high-symmetry K point.

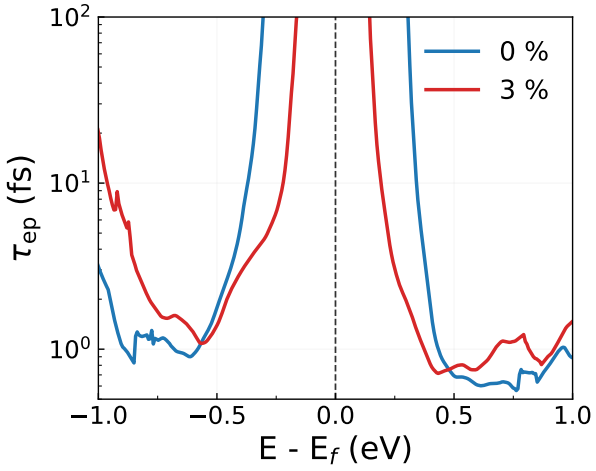

Fig. S11 Energy-dependent electron-phonon relaxation time (τ_{ep}) for unstrained and strained h−NbN at 300 K.

8 Figure of merit (zT)

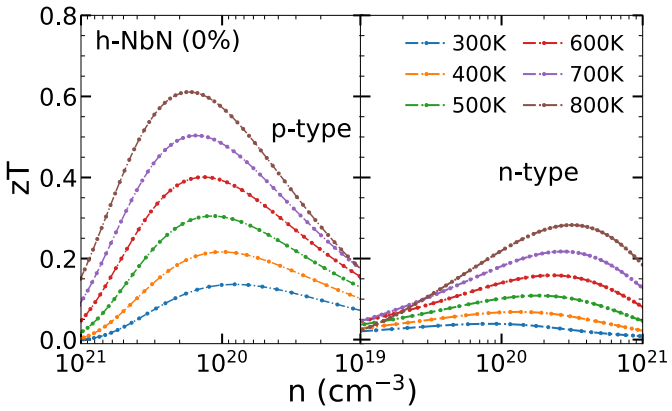

Fig. S12 Variation of the figure of merit (zT) with carrier concentration (n) for both p- and n-type at different temperatures reveals the optimal doping levels required for enhanced thermoelectric performance. The zT values are evaluated using the lattice thermal conductivity considering both three- and four-phonon scattering ($\kappa_l^{3ph+4ph}$).

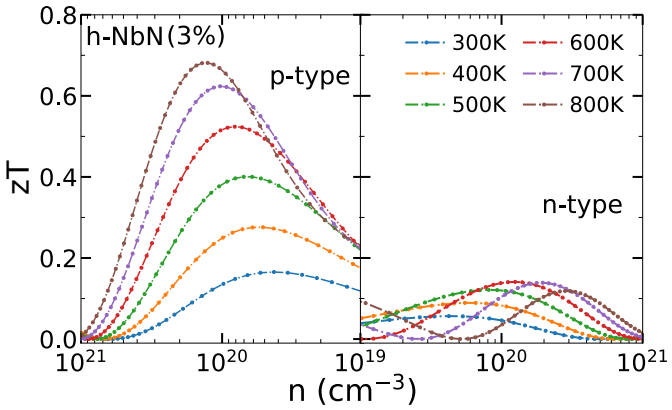

Fig. S13 Variation of the figure of merit (zT) with carrier concentration (n) for both p- and n-type at different temperatures reveals the optimal doping levels required for enhanced thermoelectric performance. The zT values are evaluated using the lattice thermal conductivity considering both three- and four-phonon scattering ($\kappa_l^{3ph+4ph}$). These results correspond to the case under 3% tensile strain.

Notes and references

1 G. Samsonidze and B. Kozinsky, *Adv. Energy Mater.*, 2018, **8**, 1800246.